IEEE Access
Multidisciplinary | Rapid Review | Open Access Journal

Received November 7, 2019, accepted November 25, 2019, date of publication November 29, 2019,
date of current version December 18, 2019.

Digital Object Identifier 10.1109/ACCESS.2019.2956832

A Study on Use of Hybrid Energy Storage System Along With Variable Filter Time Constant to Smooth DC Power Fluctuation in Microgrid

TIEZHOU WU[1], WENSHAN YU[1], AND LINXIN GUO[2]
[1]Hubei Collaborative Innovation Center for High-Efficiency Utilization of Solar Energy, Hubei University of Technology, Wuhan 430068, China
[2]Hanjiang Water Resources and Hydropower Group Company, Ltd., Danjiangkou Hydropower Plant, Danjiangkou 442700, China

Corresponding author: Wenshan Yu (yuws315@163.com)

This work was supported in part by the Technology and Device for Autonomous Cruise Cleaning and Floating and Vertical Disturbance Algae Control of Hybrid Wind and Photovoltaic Power (Research on Eutrophication Mechanism and Comprehensive Regulation and Control Technology of Channel Reservoir) through the National Key Research and Development Program under Project 2016YFC0401702.

ABSTRACT Currently, using hybrid energy storage system composed of battery and supercapacitor to stabilize DC bus power fluctuation is a hot issue. In low-pass filtering control strategy to suppress the power fluctuation of DC bus, the filtering time constant is fixed, so there are problems such as poor load power fluctuation smoothing effect and over-charge and over-discharge of the battery. In this paper, a two-stage low-pass filter control strategy with variable filter time constant is designed. Firstly, the strategy builds a multi-objective function with minimum load slow target power and DC bus power difference. Using the Improved Particle Swarm Optimisation (IPSO) with compensating coefficient of inertia weight factor to solve the optimal output power by a hybrid energy storage system, and dynamically adjust the first-level filtering time constant, in order to reduce the load power change causing the fluctuation of the DC bus power; secondly, according to the charging state of the supercapacitor and the battery, the fuzzy control method is adapted to dynamically adjust the second-order filtering time constant to optimize the power distribution of the battery and the supercapacitor. The experimental results show that the control strategy can effectively reduce the power fluctuation of DC bus by about 15%, and avoid the over limit phenomenon of the battery state of charge, which has a good prospect of engineering application.

INDEX TERMS Hybrid energy storage, power fluctuation, particle swarm optimization, low pass filter, filtering time constant.

I. INTRODUCTION

When load changes cause DC bus power fluctuation, a single energy storage device cannot better meet the requirements of high power and high energy density at the same time, which will affect the stable and reliable operation of microgrid [1]. However, hybrid energy storage system (HESS) can give full play to the complementary characteristics of battery and supercapacitor [2], which is more popular in smoothing power fluctuations of a microgrid. To improve the performance of HESS to stabilize load power fluctuation and prevent the battery from overcharging and discharging, the control strategy of the HESS in a microgrid to stabilize power fluctuation should be studied in depth [3].

The associate editor coordinating the review of this manuscript and approving it for publication was Fabio Massaro.

The control strategy of the battery-supercapacitor HESS has been studied in many articles. In ref. [4], adaptive wavelet packet decomposition was used to obtain the calming power target of the HESS, and fuzzy control method was used to optimize the power index distribution of battery and supercapacitor, to effectively improve the smoothing effect of wind power output power fluctuation. Ref. [5] proposed the optimal power control strategy of the first-order low-pass filter to avoid overcharging and over-discharging of the battery. Ref. [6] adopts fuzzy control method to optimize the charging and discharging power of the hybrid energy storage system according to the bus voltage, the frequency of the microgrid and the overall charging state of the HESS, to maintain the charging state of the energy storage equipment in a reasonable range. Ref. [7] adopts fuzzy control method to optimize the power distribution of HESS according to the supercapacitor

state of charge and gives full play to the fast dynamics of the supercapacitor to stabilize the high-frequency components of power fluctuation. Ref. [8] proposes a hybrid energy storage system composed of a high energy density battery and a high power density super capacitor to mitigate the intermittent renewable energy power fluctuations in remote areas. The experimental results show that the hybrid energy storage system can not only effectively suppress the power fluctuation of intermittent renewable energy, but also suppress the power fluctuation of the load. Ref. [9] a combination of low-pass filtering and fuzzy control strategy is proposed, which utilizes the high power density of supercapacitors, high current charge and discharge characteristics, and reduces the dynamic stress and peak current demand of the battery to prolong battery life and slow bus power fluctuation. Ref. [10] adjusted the filter time parameters of the system in real time according to the charging state of the energy storage system, realizing the long-term effective operation of the battery and supercapacitor energy storage system, but could not dynamically adjust the output power of the mixed energy storage system, effectively stabilizing the bus power fluctuation. Ref. [11] proposes a hybrid energy storage system power allocation strategy based on battery charge and discharge thresholds to limit battery charge and discharge current. This method can quickly respond to changes in wind speed and load power, but the threshold setting is relatively complicated and there is no clear method. Ref. [12] adopts the adaptive drooping technique to optimize the load distribution according to the dynamic drooping coefficient of the distributed power supply output.

In this paper, a variable filter time constant two-stage low-pass filter control strategy is designed. The strategy builds multi-objective function with minimum load slow target power and DC bus power difference, uses the Improved Particle Swarm Optimisation (IPSO) algorithm with compensating coefficient of inertia weight factor to obtain the optimal output power of the HESS, adjusts the first-level filtering time constant, in order to reduce the load power change DC bus power fluctuations. Secondly according to the supercapacitor and battery state of charge (SOC), fuzzy control method for dynamic adjustment second-level filtering time constant, optimizing the allocation of power battery and supercapacitor. The experimental results show that compared with the traditional control strategy, the control strategy can reduce the power fluctuation of DC bus by about 15%, and avoid the phenomenon of over limit of the battery SOC.

II. CONTROL STRATEGY TO STABILIZE LOAD FLUCTUATION

A. TRADITIONAL STRUCTURE AND STRATEGY OF STABILIZING LOAD FLUCTUATION

The topology of the traditional HESS to stabilize load power fluctuations is shown in figure 1. As shown in Figure 1, it is a DC micro grid, and micro power supply, hybrid energy storage system and micro grid load are connected through

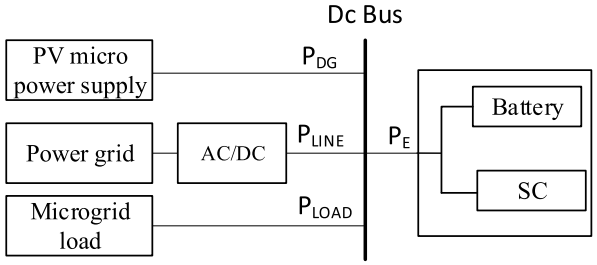

FIGURE 1. HESS topology diagram.

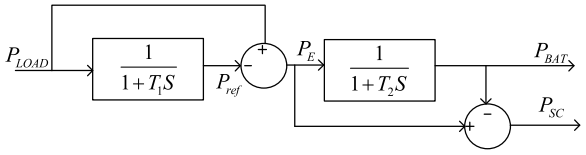

FIGURE 2. Traditional load stabilization power control strategy.

DC bus, which is connected to the grid through bidirectional AC/DC converter. P_{DG} is the output power of the PV micropower supply, P_{LINE} is the DC bus power of the microgrid, P_E is the power of the HESS, and P_{LOAD} is the power required by the load.

The traditional HESS using a two-stage low-pass filter [13] to control load changes and power distribution strategies, as shown in figure 2. P_{ref} is the external power smoothing target, S is the differential operator, T_1 is the first filtering time constant, T_2 is the second filtering time constant, P_{SC} is the power assumed by the supercapacitor in the HESS, and P_{BAT} is the power assumed by the battery in the HESS. The high-frequency components of load power fluctuation are obtained by filtering time constant T_1, and the power distribution between the supercapacitor and the battery is completed by filtering time constant T_2.

As can be seen from figure 2, although the two-stage low-pass filtering control strategy can stabilize the power fluctuation of load, the first-stage low-pass filtering HESS cannot dynamically adjust the target power of load stabilization. The output power of the HESS deviates from the actual output power, which affects the load power fluctuation stabilization. The second-level low-pass filter does not take into account the battery and the supercapacitor SOC, which will cause overcharge of the battery to in the process of utilization and affecting the service life of the HESS [14]. Among them, the battery selects the equivalent model partnership for a new generation of vehicle (PNGV), as shown in Figure 3. In Figure 3, R_P is the polarization internal resistance of the battery, R_O is the ohmic internal resistance of the battery, C_P is the polarization capacitance of the battery, C_B is the additional capacitance, indicating the change amount of the open circuit voltage generated by the accumulation of current with time change, U_{OC} is the open circuit voltage of the battery, I_L is the current passing through the equivalent ohmic internal resistance Ro. On the basis of the Thevenin equivalent model, the capacitance is added to indicate the change of the open circuit voltage with time and current

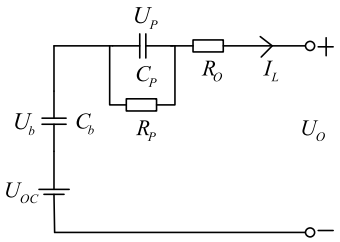

FIGURE 3. PNGV equivalent circuit model.

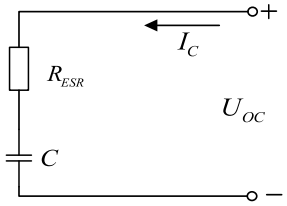

FIGURE 4. Classic RC model.

accumulation, which is more similar to the actual battery operating characteristics [15]. The super capacitor uses the classic RC model, as shown in Figure 4. In Figure 4, R_{ESR} is the equivalent resistance of super capacitor, C is the ideal capacitor, I_C is the current of super capacitor, and U_{OC} is the open circuit voltage. The model not only has a simple structure, but also has the advantages of less parameters and small calculation, and can reflect the external characteristics of the supercapacitor during charging and discharging [16].

B. IMPROVE CONTROL STRATEGY OF HYBRID ENERGY STORAGE TO STABILIZE LOAD FLUCTUATION

The two-stage low-pass filter control strategy has the problems of poor load fluctuation suppression effect and overcharge and over-discharge of the battery. In this paper, a variable filter time constant two-stage low-pass filter control strategy is designed. By building the first level low pass filtering to stabilize the output power and the multi-objective function with the smallest DC bus power load fluctuation.

It using compensation coefficient inertia weight factor of the IPSO to solve the optimal output power of HESS, dynamically adjust filtering time constant T_1, minimize the load power fluctuations. The second-level low-pass filter adopts fuzzy control method to dynamically adjust the filtering time constant T_2 according to the supercapacitor and the battery SOC to optimize the power distribution of the battery and the supercapacitor, to avoid the over-limit phenomenon of the battery SOC. Fig.5 shows the control strategy of improving hybrid energy storage to stabilize load fluctuation.

III. IPSO HYBRID ENERGY STORAGE SYSTEM TO REALIZE POWER STABILIZATION TARGETS

To overcome the insufficiency of constant filtering time constant and better adjust the power stabilization of HESS, this paper constructs a multi-objective function to minimize the fluctuation of load output power and DC bus power. IPSO algorithm is used to solve the optimal balancing power of the

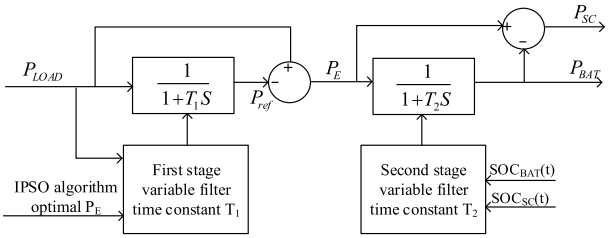

FIGURE 5. Improved load leveling power fluctuation control strategy.

HESS, and then the first stage low-pass filtering time constant T_1 is dynamically adjusted to stabilize the power fluctuation of the load effectively.

A. POWER STABILIZATION TARGET AND CONSTRAINT CONDITIONS OF THE HESS

According to the actual operation of the HESS, an objective function was established to improve the capability of the HESS to stabilize DC bus power fluctuation caused by load changes. To achieve the desired purpose of the control strategy more ideally, it makes the following provisions: the period of the control strategy was 1h, and 1h was divided into 60 periods. So, there's 60min in 1 h. The objective function is shows in equation (1).

$$\begin{cases} F_1 = \min \sum_{i=1}^{60} (P_{LINEi} - P_{LOAD_i})^2 \\ F_2 = \min[\max(P_{LINE_j}) - \min(P_{LINE_k})] \end{cases} \tag{1}$$

where P_{LOAD_i} is the load power in the microgrid. P_{LINE_i} is the power of DC bus in the microgrid. $\max(P_{LINE_j})$ is the period when the bus power is the maximum within a control strategy period. $\min(P_{LINE_k})$ is the minimum bus power period in a control strategy period.

After determining the objective function, considering the optimal performance of battery- supercapacitor and the management strategy of the energy storage system, the constraint conditions should be established according to some basic requirements of a HESS. The proposed constraints are as follows:

1) Energy conservation constraint. According to the law of conservation of energy, the output of photovoltaic power generation at a specific moment, the battery and the supercapacitor output together shall be equal to the power on the DC bus plus the grid-connected power [17]. Equation (2) is the mathematical expression. Figure 6 is the power balance diagram of microgrid.

$$P_{vi} + P_{SCi} + P_{BATi} + P_{LINEi} = P_{LOADi} \tag{2}$$

where P_{vi} is the PV micropower supply output in a certain period. P_{SC_i} is the output of the supercapacitor at a certain period. P_{BAT_i} is the output of the battery at a certain period. P_{LINE_i} is the power of busload at a certain moment, this power is provided by the grid. P_{LOAD_i} is the power of microgrid load at a certain moment.

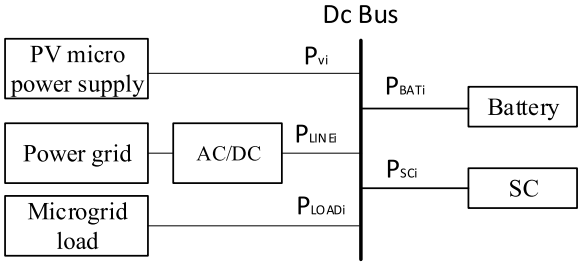

FIGURE 6. The power balance diagram of microgrid.

2) SOC constraint [18], the mathematical expression is shown in equation (3).

$$\begin{cases} 15\% \le SOC_{SC_i} \le 90\% \\ 15\% \le SOC_{BAT_i} \le 85\% \end{cases} \tag{3}$$

where SOC_{SC_i} is the supercapacitor SOC in a certain period. SOC_{BAT_i} is the battery SOC within a certain period.

Both battery and supercapacitor overcharge and over-discharge have severe effects on the life and service effect of the energy storage system. Therefore, the SOC of battery and supercapacitor need to be limited [19]. At present, the commonly used SOC estimation methods mainly include Ampere-hour integral method, Open circuit voltage method, Kalman filter method, and BP neural network method [20], [21]. The ampere-hour integral method is simple and reliable. The initial value and the sampling current can be used to estimate the battery SOC. The open circuit voltage method can be used for a variety of lithium batteries, but not for the battery SOC estimation in operation. The Kalman filter method can not only correct the system. The initial error can also effectively suppress the system noise, but the method depends on the accuracy of the battery model, and the calculation amount is large in the estimation process. The BP neural network method needs to use a large amount of historical data for training to ensure the accuracy of the estimation result. Therefore, this paper chooses the ampere-hour integral method for SOC estimation.

3) Maximum power constraint. The output power of battery and supercapacitor should not exceed their rated power. Equation (4) is the mathematical expression.

$$\begin{cases} P_{BAT_i} < P_{BAT-\max} \\ P_{SC_i} < P_{SC-\max} \end{cases} \tag{4}$$

where P_{BAT_i} is the output power of the battery for a certain period. P_{SC_i} is the output of the supercapacitor at a certain period. $P_{BAT-\max}$ is the Maximum output power for the battery. $P_{SC-\max}$ is the maximum output power for the supercapacitor.

B. IMPROVEMENT AND VERIFICATION OF THE PSO ALGORITHM

PSO algorithm is a global optimization algorithm based on swarm intelligence heuristic [22]. The core idea of the algorithm is to determine and adjust the direction and size of the next search by referring to the individuals in the optimal position in the group and the optimal position reached by the particle. Its mathematical expression is shown in equation (5).

$$\begin{cases} x_{id} = x_{id} + v_{id} \\ v_{id} = wv_{id} + c_1 r_1 (p_{id} - x_{id}) + c_2 r_2 (p_{gd} - x_{id}) \end{cases} \tag{5}$$

where c_1 is the learning factor. c_2 is the learning factor. r_1 is the random number between (0,1). r_2 is the random number between (0,1). w is the inertia weighting factor.

Each particle i has a dimensional position vector ($x_i = x_{i1}, x_{i2} \ldots\ldots x_{id}$) and velocity vector ($v_i = v_{i1}, v_{i2} \ldots \ldots v_{id}$). In the initial stage of the algorithm, each particle will distribute randomly into space, and then the fitness of each particle in the current position will be calculated. Before each iteration, each particle adjusts and calculates the velocity vector and position of the particle according to its inertia, experience and the position experienced by the optimal value of the population until the best place P_{best} is found.

However, in the process of getting the solution, although the traditional PSO algorithm has the advantage of fast convergence speed, there is a phenomenon called "precocity." When a particle is in the optimal local solution, other surrounding particles will quickly approach the particle, making the algorithm fall into the local optimal solution [23]. Secondly, the value of the algorithm also has a significant impact on the results of the algorithm, and the large w is conducive to the rapid convergence of the algorithm, the small w is helpful to the algorithm to improve the search accuracy. Combined with the actual work of the HESS, it adds a self-adjusting strategy that set the maximum number of local search iterations.

After the specified number of iterations, if the population still fails to meet the requirements of system error, the current state shall be saved, and the particles near the optimal local solution shall be initialized and searched again. The inertia weight factor of the PSO algorithm is modified according to formula (6) to increase the compensation coefficient. When the particle is far away from the optimal global value, the improved value can make the search speed faster and accelerate the convergence of the system. When the particle is close to the optimal global value, the value decreases and the search precision is improved.

$$w = \begin{cases} w' + k' \dfrac{dv_{id}}{dt} & g'_{\text{best}} > \Delta\text{error} \\ w' - k'' \dfrac{dv_{id}}{dt} & g'_{\text{best}} < \Delta\text{error} \end{cases} \tag{6}$$

where w' is the reference value of w. k'' is the compensation coefficient. k' is the compensation coefficient. v_{id} is the velocity of the current particle. Δ_{error} is the allowable error of the system.

To verify the optimization function of IPSO, it uses four standard functions as objective functions [24]. After calculating the corresponding adaptive values, they are compared with PSO. The four test functions are:

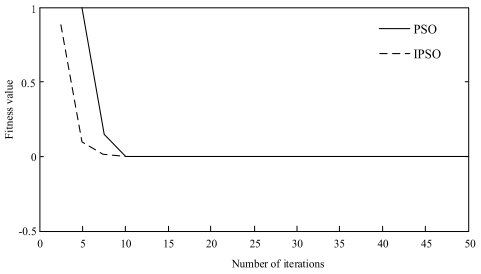

FIGURE 7. Sphere function.

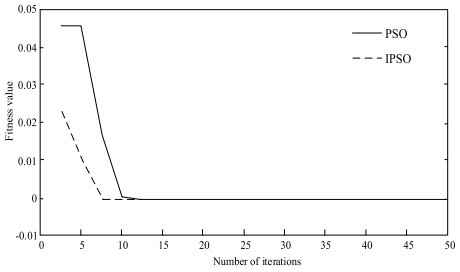

FIGURE 8. Griewank function.

(1) Sphere function:

$$f_1(x) = \sum_{i=1}^{n} x_i^2 \tag{7}$$

(2) Griewank function:

$$f_2(x) = \frac{1}{4000}\sum_{i=1}^{n} x_i^2 - \sum_{i=1}^{n} \cos\left(\frac{x_i}{\sqrt{i}}\right) + 1 \tag{8}$$

(3) Ackley function:

$$f_3(x) = -20e^{-0.2\sqrt{\frac{1}{n}\sum_{i=1}^{n} x_i^2}} - e^{\frac{1}{n}\sum_{i=1}^{n}\cos(2\pi x_i)} + 22.71282 \tag{9}$$

(4) Rastrigrin function:

$$f_4(x) = \sum_{i=1}^{n}\left[x_i^2 - 10\cos(2\pi x_i) + 10\right] \tag{10}$$

where x_i is the value of the independent variable of the function.

In equations (7), (8), (9) and (10), $f_1(x)$ is a single-peak function, and the theoretical minimum is 0; $f_2(x)$ gets the global minimum at $x_i = 0(i = 1, 2, \ldots n)$; to obtain the global minimum; there are many local extrema points off $f_4(x)$, but only one global minimum $f_{\min} = 0$.

In IPSO, the learning factor is C1 = 1.5 and C2 = 1.5, and refers to a random number, the inertial weight is modified according to formula (6), the number of particle swarm: N = 40, the search dimension: d = 4 and the maximum amount is 100 iterations. PSO and IPSO run 50 times in each objective function, and the corresponding function iteration results are show in figure 7, figure 8, figure 9 and figure 10.

According to the analysis in Fig. 7, Fig. 8, Fig. 9 and Fig. 10, when the function reaches the optimal value, the iteration number of IPSO is less than PSO, and the adaptive value

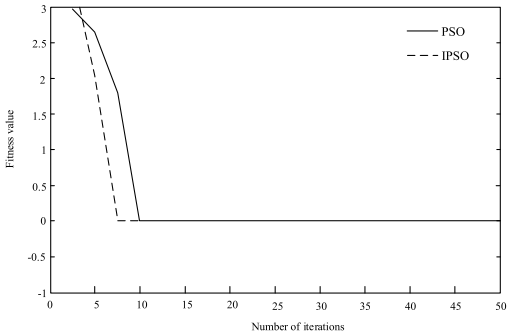

FIGURE 9. Ackley function.

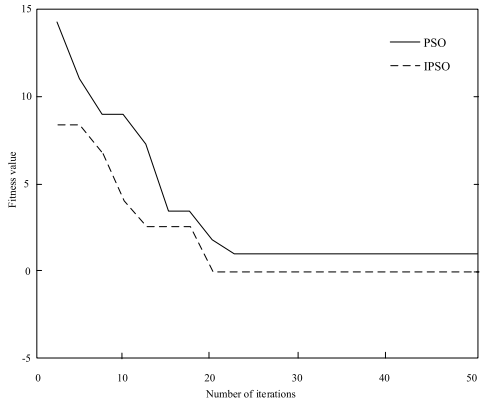

FIGURE 10. Rastrigrin function.

of the objective function is less than PSO. For the solutions with multiple local minima, such as the Rastrigrin function, PSO algorithm is prone to get caught in the optimal local solution, while IPSO algorithm shows better performance regarding searchability, accuracy and convergence speed, which proves the correctness of IPSO algorithm.

C. SOLVING PROCESS BASED ON IPSO ALGORITHM

There are two objective functions which are needed to be processed in the system. The traditional method is to introduce the proportional coefficient, consider the impact of each objective function on particle flight, determine the proportional coefficient. However, this method cannot accurately search for the optimal global value, and when the number of objective functions increases further, as this method requires a large amount of calculation to determine the proportional coefficient, it will lead to further error expansion.

Therefore, in this paper, the method of integral solution is used to jointly guide the flight of each particle in the decision variable space through the multi-objective function. Due to the existence of multiple objective functions, particles do not move in the direction of the function, nor the direction of the function, but in a certain direction between the function and the function, so that they eventually fall into the non-inferior optimal solution. The specific process is as follows:

1) Firstly, find the extreme global values of each target function corresponding to each particle. In this case, $G_{best}[1]$ and $G_{best}[2]$ should be observed.

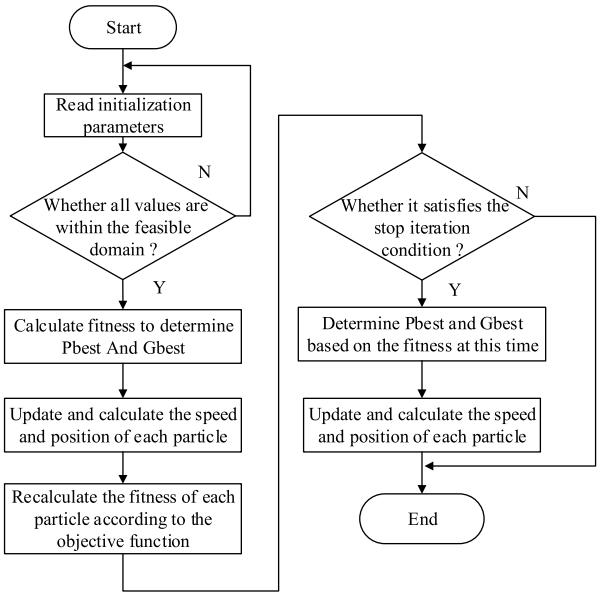

FIGURE 11. Flowchart of algorithm solution.

2) Then find the individual extreme values of each target function corresponding to each particle in the processing. In this case, $P_{best}[1, i]$ and $P_{best}[2, j]$ should be found. $P_{best}[1, i]$ is the individual extreme value of the i particle in the first objective function. $P_{best}[2, j]$ is the individual extreme value of the j particle in the second objective function.

3) When the algorithm starts $G_{best}[1]$ and $G_{best}[2]$ will be the "default" value. When the speed of each particle needs to be updated, it can judge the individual extreme value of each particle by comparing the individual extreme value of the particle with the "default" value. Determining whether to select the updated position or to select a random value from the individual extreme value.

After several iterations, the global optimal value under multiple objective functions can be determined.

The solution flowchart of the algorithm is shown in figure 11.

IV. OPTIMAL POWER DISTRIBUTION STRATEGY BASED ON THE FUZZY CONTROL METHOD

A. CALCULATION METHOD OF VARIABLE FILTER TIME CONSTANT BASED ON FUZZY CONTROL

To consider the charge state of each energy storage unit in the power distribution of the HESS, the fuzzy control strategy is adopted in this paper to adjust the second-order filtering time constant to optimize the power distribution of the energy storage system [25]. The charged state of the battery SOC_{BAT} and the supercapacitor SOC_{SC} are two important constants that affect the filtering time constant. After normalization, variables $X_{BAT-SOC}(t)$ and $X_{SC-SOC}(t)$ can be obtained:

$$X_{BAT-SOC}(t) = \frac{SOC_{BAT}}{SOC_{BAT0}} - 1 \tag{11}$$

$$X_{SC-SOC}(t) = \frac{SOC_{SC}}{SOC_{SC0}} - 1 \tag{12}$$

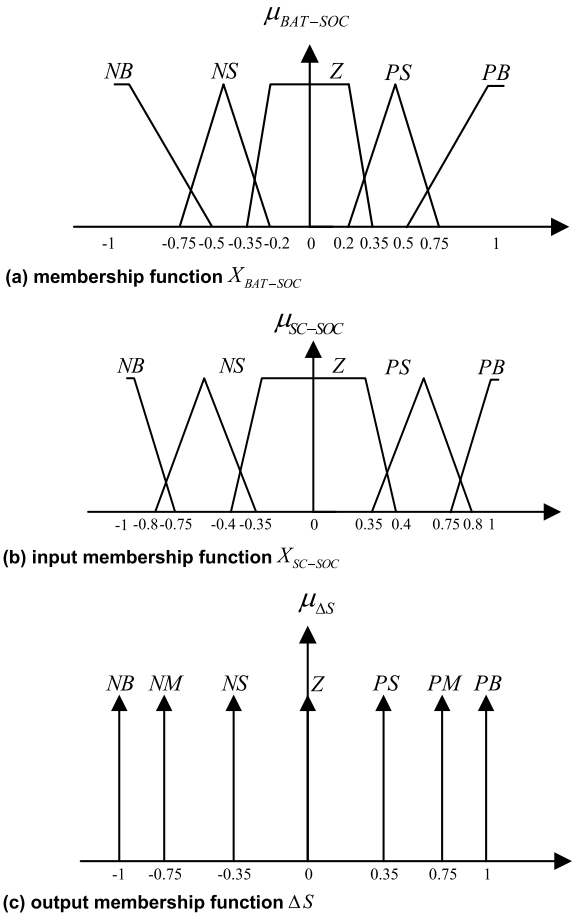

FIGURE 12. Input and output membership functions.

where SOC_{BAT0} is the median of the charged state of the battery. SOC_{SC0} is the median of the charged state of the supercapacitor.

In this paper, $X_{BAT-SOC}(t)$ and $X_{SC-SOC}(t)$ is taken as the input of fuzzy control and filter time constant correction is considered as the output to construct a two-dimensional fuzzy controller with two inputs and one output. The input membership function and output membership degree function are shown in figure 12. As shown in Figure 12, the fuzzy set of $X_{BAT-SOC}(t)$ is {NB (negative big), NS (negative small), Z (zero), PS (positive small), PB (positive small)}; the fuzzy set of $X_{SC-SOC}(t)$ is {NB (negative big), NS (negative small), Z (zero), PS (positive small), PB (positive small)}; and the fuzzy set of $\Delta S(t)$ is {NB (negative big), NM (negative middle), NS (negative small), Z (zero), PS (positive small), PM (positive middle), PB (positive small)}. Through the fuzzy set, the precise deviation of variables can be transformed into the fuzzy language that can be recognized by the fuzzy control.

The choice of membership function is often based on experience and the nature of variables themselves. For example, for variable $X_{BAT-SOC}(t)$, it is obvious that when SOC of lithium-ion battery is in (0.4, 0.6), we think it is in Z (median) region of SOC, so the membership function is horizontal

TABLE 1. Fuzzy control rules under charging state.

		$X_{BAT-SOC}(t)$				
		NB	NS	Z	PS	PB
$X_{SC-SOC}(t)$	NB	Z	NS	NM	NB	NB
	NS	PS	Z	NS	NM	NB
	Z	PM	PS	Z	NS	NM
	PS	PB	PM	PS	Z	NS
	PB	PB	PB	PM	PS	Z

TABLE 2. Fuzzy control rules under discharging state.

		$X_{BAT-SOC}(t)$				
		NB	NS	Z	PS	PB
$X_{SC-SOC}(t)$	NB	Z	PS	PM	PB	PB
	NS	NS	Z	PS	PM	PM
	Z	NM	NS	Z	PS	Z
	PS	NB	NM	NS	Z	Z
	PB	NB	NB	NM	NS	Z

straight line (− 0.2, 0.2), and when SOC is in (0.6, 0.675), the probability of belonging to Z decreases gradually, while the probability of belonging to PS increases gradually, so it presents inclined straight line. The membership functions of $X_{SC-SOC}(t)$ and $\Delta S(t)$ can be determined from this.

According to the corresponding fuzzy subset of input $X_{BAT-SOC}(t)$ and $X_{SC-SOC}(t)$ the corresponding fuzzy control, rules are established. When the mixed energy storage output power is $P_E > 0$ (charging state), the fuzzy control rules under charging state are shown in table 1. When the output power of mixed energy storage $P_E < 0$ (discharge state), the fuzzy control rules under discharge state are shown in table 2. The charging state could illustrate: if the battery and the supercapacitor SOC are the intermediate values, the preset time constant remains unchanged; If the battery SOC is close to the lower limit and the supercapacitor SOC is close to the upper limit, the time constant T is appropriately increased to increase the charging power of the battery. If the battery SOC is close to the upper limit and the supercapacitor SOC is close to the lower limit, the time constant T is appropriately reduced to increase the charging power of the supercapacitor. If both the battery and the supercapacitor SOC are in the lower limit, increase the time constant T appropriately and give priority to improving the charging power of the battery to ensure the regular discharge of the battery at the next moment.

The center of gravity method was used to solve the fuzzy set of output [26], and the correction coefficient $\Delta S(t)$ of filtering time constant at time t was calculated:

$$\Delta S(t) = \frac{\sum_i \sum_j \mu_{1i}(SOC_{BAT})\,\mu_{2j}(SOC_{SC})\,\Delta S_{ij}}{\sum_i \sum_j \mu_{1i}(SOC_{BAT})\,\mu_{2j}(SOC_{SC})} \quad (13)$$

where $\mu_{1i}(SOC_{BAT})$ is the i-th membership value of the input quantity $X_{BAT-SOC}(t)$. $\mu_{2j}(SOC_{SC})$ is the j-th membership value of the input quantity. ΔS_{ij} is the input corresponding output quantity of $X_{BAT-SOC}(t)$ and $X_{SC-SOC}(t)$.

The modified filtering time constant is $T' = T(1 + \Delta S(t))$.

B. OPTIMAL POWER DISTRIBUTION CONTROL STRATEGY

According to the SOC of the battery and the supercapacitor, the second-level low-pass filter is used to optimize the power distribution of the HESS, and the output power of the battery and the supercapacitor is obtained [27]. The necessary steps are as follows:

(1) Set the second-level low-pass filtering time constant T_2 and sampling period, and use equation (14) to obtain the initial power instruction of the battery at the current moment;

$$P_{BAT-0}(t) = \frac{T_2}{T_2 + \Delta t} P_{BAT}^{t-\Delta t} + \frac{\Delta t}{T_2 + \Delta t} P_E \quad (14)$$

(2) According to battery SOC and supercapacitor SOC, the current variable filter time constant $T_2' = T_2(1 + \Delta S(t))$ is calculated by the fuzzy control method.

(3) By using the variable filter time constant, the power instruction of the modified battery $P_{BAT}(t)$ is calculated again.

(4) The power instruction of the supercapacitor is obtained from formula (15) to realize the optimal power distribution.

$$P_{SC}(t) = P_E - P_{BAT} \quad (15)$$

According to the battery SOC and supercapacitor SOC, the fuzzy control method is utilized to dynamically adjustment filtering time constant, which can make the HESS fully consider the battery SOC and supercapacitor SOC during power distribution, rectifying initial HESS power allocation instruction and keeping the battery SOC within a reasonable range, avoiding battery overcharge and over-discharge occurrence [28]. In the actual operation process, the low-pass filter time constant can be adjusted by adjusting the capacitance value of the low-pass filter.

V. CASE ANALYSIS

To verify the correctness of the IPSO algorithm's HESS smoothing power target and the fuzzy control method's power optimal allocation strategy, experiments were carried out. The power demand fluctuation on the microgrid DC bus is sampled. The capacity allocation of the hybrid energy storage system used in this experiment is obtained by the method proposed in reference [29]. As shown in Figure 13, the experimental platform is built. In the figure, DC load is directly connected to DC bus, lithium-ion battery and super capacitor are included into DC bus through DC / DC, and outdoor photovoltaic modules and power grid are connected to DC bus through DC / DC and AC / DC respectively. The parameters are set as follows (Table 3):

The battery pack consists of a 48 V, 40 Ah lithium iron phosphate battery module 6 string 2, and the supercapacitor group consists of a 54 V, 17.5 F single supercapacitor 7 string 2, and the battery pack and the supercapacitor group pass the DC/DC module respectively. The microgrid DC bus is connected. Low pass filtering initial time constant $T_2 = 50$ s. The power smoothing object is the microgrid power plant of 100 kW. The typical DC bus power demand curve is shown in Figure 14, in the sampling period of

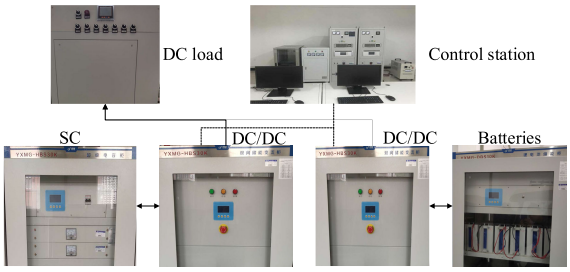

FIGURE 13. Experimental platform.

TABLE 3. Experimental platform construction design index.

parameter name	Parameter value
Operating temperature	TC=25oC
DC bus rated voltage	VDC=500 V
PV rated output	100kW
Battery rated voltage	VBAT=288 V
Battery rated capacity	480 Ah
Battery initial SOC	SOC=60%
Supercapacitor rated voltage	VSC=378 V
Supercapacitor rated capacity	5 F
Transmission efficiency	0.95

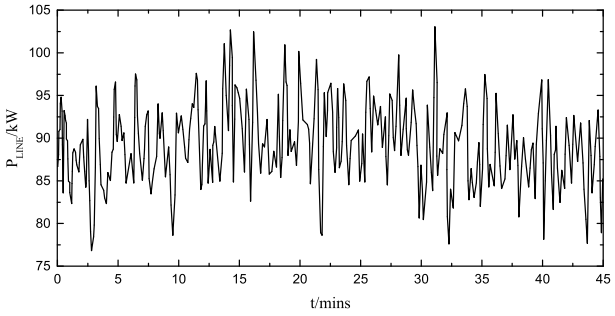

FIGURE 14. Power demand fluctuation diagram on DC bus.

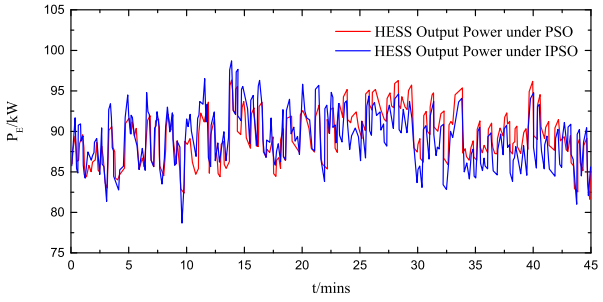

FIGURE 15. Comparison of the output power of a HESS.

45 minutes, the maximum power requirement is 105 kW, the minimum power requirement is 73 kW.

By applying PSO and IPSO to the microgrid system for comparison experiment, the output power comparison of the HESS is shown in figure 15. As can be seen from figure 15, the overall output power fluctuation of the HESS is smaller than that of IPSO. This is because PSO is prone to fall into the local optimal solution when solving the optimal output power of the HESS, failing to accurately obtain the optimal power output of the HESS and controls the load power fluctuation.

After getting the optimal output power HESS, whether the variable filter time constant of the low-pass filter control strategies have energy storage unit charging state need to

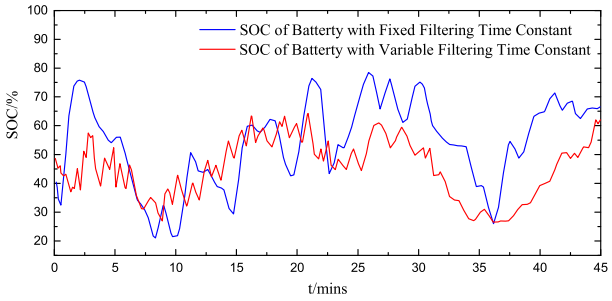

FIGURE 16. SOC change of battery.

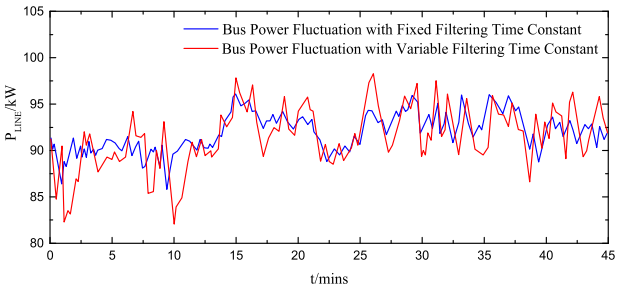

FIGURE 17. Power fluctuation of DC bus after using this control strategy.

be determined. Then filtering time constant is dynamically adjusted, power allocation of the HESS is optimized, thus achieving the control of load power fluctuations and keeping the battery SOC values within a reasonable range and avoiding overcharge and over discharge.

As shown in figure 16, before the proposed control strategy is add to the HESS, the SOC of the battery changed significantly and times of exceeding the limit appeared. After using the variable filter time constant control strategy, the SOC change range of the battery is significantly reduced, and the SOC value is within the limit range, thus avoiding the over-charging and over-discharging of the battery in the working process.

Figure 17 shows the power fluctuation on the DC bus using the proposed control strategy. Compared with the fluctuation of DC bus power demand, not only the fluctuation of the power curve is stabilized, but also the fluctuation rate of DC bus power is significantly reduced. Comparing Figures 10 and 13, the fluctuation of power on DC bus is reduced from 15 kW to less than 10 kW, which reduces the fluctuation rate of DC bus by about 15%.

VI. CONCLUSION

In this paper, a two-stage low-pass filter control strategy with variable filter time constant is used. Firstly, a multi-objective function is constructed to suppress the minimum difference between the target power and the DC bus power, and IPSO is used to solve the optimal output power of the HESS. Then, the first filter time constant is dynamically adjusted to reduce the DC bus power fluctuation caused by the change of load power. The fuzzy control method is used to dynamically improve the second filter time constant and optimize the power distribution of the supercapacitor and

the battery. The experimental results show that compared with the traditional control strategy, the control strategy reduces the fluctuation rate of DC bus power by about 15%, and effectively suppresses the over-limit phenomenon of battery charging state.

REFERENCES

[1] W. Ning and Z. Jiancheng, "Capacity allocation method of hybrid energy storage system based on energy coordination control," *Electr. Power Construct.*., vol. 37, no. 8, pp. 72–77, Aug. 2016.

[2] J. Du, X. Zhang, T. Wang, Z. Song, X. Yang, H. Wang, M. Ouyang, and X. Wu, "Battery degradation minimization oriented energy management strategy for plug-in hybrid electric bus with multi-energy storage system," *Energy*, vol. 165, no. 1, pp. 153–163, Dec. 2018.

[3] J. Xiao, P. Wang, and L. Setyawan, "Multilevel energy management system for hybridization of energy storages in DC microgrids," *IEEE Trans. Smart Grid*, vol. 7, no. 2, pp. 847–856, Mar. 2016.

[4] W. Jie and D. Ming, "Hybrid energy storage using adaptive wavelet packet decomposition to control wind power fluctuation control strategy," *Autom. Electr. Power Syst.*, vol. 41, no. 3, pp. 7–12, Feb. 2017.

[5] C.-L. Nguyen and H.-H. Lee, "Power management approach to minimize battery capacity in wind energy conversion systems," *IEEE Trans. Ind. Appl.*, vol. 53, no. 5, pp. 4843–4854, Sep./Oct. 2017.

[6] L. Hui, H. Yaomei, and M. Fei, "Coordinated control strategy for hybrid energy storage system based on state of charge," *China Electr. Power.*, vol. 50, no. 1, pp. 158–163, Jan. 2017.

[7] G. Jinjin and W. Hongbin, "Hybrid storage energy coordination optimization control method for suppressing wind power fluctuations," *J. Solar Energy*, vol. 37, no. 10, pp. 2695–2702, Dec. 2016.

[8] T. Ma, H. Yang, and L. Lu, "Development of hybrid battery–supercapacitor energy storage for remote area renewable energy systems," *Appl. Energy*, vol. 153, no. 1, pp. 56–62, Sep. 2015.

[9] L. W. Chong, Y. W. Wong, R. K. Rajkumar, and D. Isa, "An optimal control strategy for standalone PV system with battery-supercapacitor hybrid energy storage system," *J. Power Sources*, vol. 331, no. 1, pp. 553–565, Nov. 2016.

[10] S. Chunjun, N. Chunhua, and D. Xiaobo, "Hybrid energy storage optimization strategy based on SOC state feedback," *Electr. Measuring Instrum.*, vol. 53, no. 15, pp. 81–88, Aug. 2016.

[11] T.-L. Pan, H.-S. Wan, and Z.-C. Ji, "Stand-alone wind power system with battery/supercapacitor hybrid energy storage," *Int. J. Sustain. Eng.*, vol. 7, no. 2, pp. 103–110, Mar. 2014.

[12] S. Augustine, M. K. Mishra, and N. Lakshminarasamma, "Adaptive droop control strategy for load sharing and circulating current minimization in low-voltage standalone DC microgrid," *IEEE Trans. Sustain. Energy*, vol. 6, no. 1, pp. 132–141, Jan. 2015.

[13] B. Xiaohui, S. Wei, and M. Rui, "Control strategy and switching optimization of hybrid energy storage system in optical storage microgrid," *J. Chongqing Univ.*, vol. 39, no. 6, pp. 11–18, Jun. 2016.

[14] W. Haibo, X. Luguang, and Y. Xiu, "Control strategy of independent photovoltaic system considering mixed charge state of charge," *Electr. Measuring Instrum.*., vol. 53, no. 15, pp. 39–46, Sep. 2016.

[15] Q. Wang, J. Wang, P. Zhao, J. Kang, F. Yan, and C. Du, "Correlation between the model accuracy and model-based SOC estimation," *Electrochim. Acta*, vol. 228, pp. 146–159, Feb. 2017.

[16] H. Xiao-Bin, Z. Xiong, and W. Tong-Zhen, "Development and applications status of supercapacitors," *Adv. Technol. Electr. Eng. Energy*, vol. 9, no. 11, pp. 63–70, Nov. 2017.

[17] L. Peng, Y. Tianmeng, and Q. Suhua, "Optimized configuration of microgrid hybrid energy storage capacity based on spectrum Analysis," *Power Syst. Technol.*, vol. 40, no. 2, pp. 376–381, Feb. 2016.

[18] L. Peiqiang, L. Wenying, and T. Jie, "Hybrid energy storage based on SOC optimization to reduce wind power fluctuation method," *Electr. Power Syst. Automat.*, vol. 29, no. 3, pp. 20–27, Apr. 2017.

[19] J. Liu and L. Zhang, "Strategy design of hybrid energy storage system for smoothing wind power fluctuations," *Energies*, vol. 9, no. 12, p. 991, Nov. 2016.

[20] J. Bo and L. I. Xiaoming, "Estimation of the residual capacity of storage batteries installed on metro train," *Urban Mass Transit.*, vol. 19, no. 12, pp. 66–68, May 2016.

[21] J. Meng, M. Ricco, G. Luo, M. Swierczynski, D.-I. Stroe, A.-I. Stroe, and R. Teodorescu, "An overview and comparison of online implementable SOC estimation methods for lithium-ion battery," *IEEE Trans. Ind. Appl.*, vol. 54, no. 2, pp. 1583–1591, Mar./Apr. 2018.

[22] B. Gordan, D. J. Armaghani, M. Hajihassani, and M. Monjezi, "Prediction of seismic slope stability through combination of particle swarm optimization and neural network," *Eng. Comput.*, vol. 32, no. 1, pp. 85–97, 2016.

[23] M. Taherkhani and R. Safabakhsh, "A novel stability-based adaptive inertia weight for particle swarm optimization," *Appl. Soft. Comput.*, vol. 38, pp. 281–295, Jan. 2016.

[24] W. Dong, L. Kang, and W. Zhang, "Opposition-based particle swarm optimization with adaptive mutation strategy," *Soft Comput.*, vol. 21, no. 17, pp. 5081–5090, Sep. 2017.

[25] Y. Yanjie, S. Ruoyu, and Z. Chaochuan, "A study on energy management strategy of hybrid energy storage system based on fuzzy control," *Renew. Energy*, vol. 35, no. 12, pp. 1881–1887, Dec. 2017.

[26] A. Hussain, V.-H. Bui, and H.-M. Kim, "Fuzzy logic-based operation of battery energy storage systems (BESSs) for enhancing the resiliency of hybrid microgrids," *Energies*, vol. 10, no. 3, p. 271, Feb. 2017.

[27] S. Jinxiao, H. Wenbiao, and Q. Nengling, "Power fluctuation-suppression strategy for distributed renewable energy in electro-thermal combined microgrid," *Proc. CSEE*, vol. 38, no. 2, pp. 537–546, Jan. 2018.

[28] J.-H. Cho, M.-G. Chun, and W.-P. Hong, "Structure optimization of standalone renewable power systems based on multi object function," *Energies*, vol. 9, no. 8, p. 649, Aug. 2016.

[29] H. Wang, T. Wang, X. Xie, Z. Ling, G. Gao, and X. Dong, "Optimal capacity configuration of a hybrid energy storage system for an isolated microgrid using quantum-behaved particle swarm optimization," *Energies.*, vol. 11, no. 2, pp. 454–468, Feb. 2018.

TIEZHOU WU was received the B.S. degree in radio and information engineering from Wuhan University, China, in 1988, and the M.S. degree in engineering from Naval Engineering University, China, in 2003, and the Ph.D. degree in systems analysis and integration from the Huazhong University of Science and Technology, China, in 2010. He is currently the Executive Vice-President of the Solar Energy Research Institute, Hubei University of Technology, and Collaborative Innovation Center of Hubei Province for efficient utilization of solar energy, and the Director of the Key Laboratory of Solar Power Generation And Energy Storage Operation Control. He is also engaged in energy storage technology, photovoltaic power generation technology, system analysis, and integration.

WENSHAN YU was born in Zhongxiang City, China, in 1995. He received the B.S. degree in electronic information engineering from the Hubei University of Technology, in 2017, and the Ph.D. degree in mechanical engineering from Drexel University, Philadelphia, PA, USA, in 2008. He is currently pursuing the M.S. degree with Power Electronics and Power Drive, Hubei University of Technology, Wuhan, China. His current research interests include renewable energy generation, electrochemical energy storage system capacity configuration and energy storage system control strategy.

LINXIN GUO received the B.S. degree in electrical engineering and automation from Luojia College, Wuhan University, China, in 2016, and the M.S. degree in electrical engineering from the Hubei University of Technology, China, in 2019. He is currently the probationary duty officer with the Hanjiang Water Resources & Hydropower Group Co., Ltd., Danjiangkou Hydropower Plant. He is also engaged in Operation Management of Power Plant and energy storage technology.